Influence of alkali content and silica modulus on the carbonation kinetics of alkali-activated slag concrete

Olivera Bukvic[1], *Marijana* Serdar[1,*]

[1]Department of materials, Faculty of Civil Engineering, University of Zagreb, Croatia

Abstract. Carbonation is inevitable process during the service life of concrete structures, where CO_2 causes decalcification of the calcium-bearing phases. These changes affect the durability of concrete and accelerate the corrosion of reinforcement. Alkali-activated materials (AAMs) are alternative, cement-free binders based on aluminosilicate rich precursor and alkaline activator. The interest in AAMs increased during the last century, due to the production process with low CO_2 footprint comparing to Portland cement (PC) concrete, the possibility to use wide range of industrial by-products as precursors and comparable performance to PC concrete. Despite the extensive research in this field, the carbonation resistance of AAMs needs to be better understood, due to the differences and complexity of binder chemistry compared to PC concrete. The propagation of carbonation process will depend on chemical composition of the precursors and the type and dosage of activators. This paper presents the results of microstructural changes of three alkali-activated concrete mixes after exposure to accelerated carbonation. Ground granulated blast furnace slag was used as a precursor and sodium hydroxide and sodium silicate as activators. Three mixes have constant water to binder ratio and slag content, while alkali content and silica modulus were varied. The carbonation resistance was evaluated by testing carbonation depth after 7 and 28 days of exposure in carbonation chamber. Microstructural changes during carbonation were investigated by thermogravimetric analysis and mercury intrusion porosimetry.

1 Introduction

Alkali- activated materials (AAMs) are binders based on aluminosilicate rich precursors and alkaline activators. AAMs can be synthesized from a range of industrial by-products as precursors, such as various types of slags or fly ash, resulting in cement-free binders with a low CO_2 footprint compared to Portland cement (PC) concrete [1]. The alkaline activation reaction is set off by the activators, e.g., alkali hydroxide, silicate, carbonate or sulphate solutions [2]. AAMs can be designed to have similar properties to PC concrete. However, this depends on the chemical composition and physical properties of precursors and chemistry and dosage of the activators. Therefore, the complexity of binder chemistry leads to a wide variety of properties and difficulties in predicting the long-term durability of AAMs [3].

During service life, concrete structures are inevitably exposed to the carbonation process along with other environmental factors. The CO_2 from the atmosphere reacts with the hydration products and leads to the decalcification of the calcium-rich hydration products, the decrease of the alkalinity of the pore solution, and the acceleration of the corrosion of the steel reinforcement [4]. The reaction products in AAMs differ from the hydration products of PC concrete and depend on the Ca content in precursors [4]. The main hydration product of slag-based AAMs is calcium alumino silicate hydrate (C-A-S-H) gel, while the secondary products are hydrotalcite and Aluminate-Ferrite-mono (sulphate) hydrate phases [4-6]. AAMs have been reported to be more susceptible to carbonation than PC concrete [7], especially under accelerated carbonation conditions with high CO_2 concentration at controlled relative humidity [3,8]. However, their high pore solution pH after natural carbonation may be promising with respect to reinforcement corrosion [9]. Their resistance to carbonation depends mainly on the properties of hydration products, pore structure, and pore solution chemistry, which are determined by the chemistry of the precursor and the dosage and type of activator [3,7]. Conflicting results have been reported regarding which type of activator best promotes carbonation resistance [10]. Despite the increasing scientific and commercial interest in AAMs for decades, there are still open

*Corresponding author: marijana.serdar@grad.unizg.hr

questions regarding the mix design of AAMs to achieve satisfactory carbonation resistance.

It is reported that higher alkali content (%Na_2O) and higher silica modulus (Ms) of the mix (i.e., SiO_2/Na_2O) improve the carbonation resistance [3,11,12]. A higher alkali content may result in higher activation degree of the slag, while a higher Ms results in a denser matrix and lower permeability due to slower slag hydration, which in turn results in a more uniform distribution of hydration products [3,6,10]. It is believed that the volumetric expansion of hydrotalcite during hydration decreases matrix porosity of AAMs and CO_2 diffusion [13]. In addition, the ability of hydrotalcite to absorb CO_2 may increase carbonation resistance [3,14]. It has been reported that slag activation with higher alkali dosage results in formation of more hydrotalcite-like phases, which can absorb more CO_2 [3,14,15]. However, when the alkali dosage is too high (e.g., 10%), not all Na_2O contributes to the activation reaction and may increase the carbonation depth due to carbonation-induced cracking [15].

This paper presents the results of the analysis of the microstructural changes of three alkali-activated slag concrete mixes with different alkali content and silica modulus after exposure to accelerated carbonation. Alkali content and Ms were dosed to attain three compressive strength classes: C25/30, C30/37, and C40/50. Although it is discussed in the literature that accelerated carbonation testing overestimates the susceptivity of AAMs to carbonation [8,16], it is used in this study for a comparative analysis to gain insight into the durability of AAM mixes of different compressive strength classes.

2 Materials and methods

2.1 Raw materials

The GGBFS precursor (supplied by Ecocem Benelux) was activated with sodium hydroxide and sodium silicate in all three AAM mixes. The chemical composition of the slag determined by X-ray fluorescence is presented in Table 1. The sodium hydroxide solution was prepared by dissolving NaOH pellets in water. The commercially available sodium silicate solution Geosil 34417, produced by Woellner was used, with a molar ratio of 1.7 and the following chemical composition: Na_2O = 16.7%, SiO_2 = 27.5%, H_2O = 55.8%. Crushed limestone aggregates with a maximum particle size of 16 mm and a ratio of fine to coarse aggregate of 1:1.5 were used for the mixes.

2.2. Mix design and sample casting

The GGBFS content and water to binder ratio (w/b) of the three AAM mixes (i.e., S1, S2 and S3) were kept constant, while the alkali content and Ms were varied to attain targeted compressive strength classes. Total water was calculated as the sum of water in activators and tapped water added to obtain the satisfactory consistence. Total solids in w/b ratio are equal to the sum of slag, sodium hydroxide pellets and solids in sodium silicate. Alkali content was calculated as the sum of Na_2O in sodium hydroxide and sodium silicate, expressed as wt% GGBFS. The mix design and compressive strength for the AAM mixes is presented in Table 2.

The cast 150 mm cube samples were demoulded after 24 hours and cured for 28 days sealed in polymeric films.

2.3. Methods

The compressive strength of the mixes was tested according to EN 12390-3 after 28 days of curing.
Accelerated carbonation testing was performed as described in EN 12390-12. After 28 days of curing, prior to placing in carbonation chamber, unsealed samples were stored under laboratory conditions (i.e., temperature 18-25°C and RH 50-65%) for 14 days. Carbonation depth was determined by the phenolphthalein spray method on two samples of each mix after they were exposed to accelerated carbonation conditions for 7 and 28 days, i.e., 3% CO_2 at 20°C and RH 57%. The samples were split in half and sprayed with phenolphthalein.

Thermogravimetric analysis (TGA) was performed using the TGA 55 instrument (TA Instruments), by heating approximately 50 mg of samples form 30ºC to 1000ºC, with a constant heating rate of 10ºC/min, in nitrogen atmosphere. Carbonated powder was extracted from the cube samples after 7 and 28 days of exposure in carbonation chamber. For the comparison, the powder was extracted from samples unexposed to accelerated carbonation (i.e., after 28 days of sealed curing and an additional 14 days under laboratory conditions).

Table 1. Chemical composition of GGBFS

Oxide	SiO_2	Al_2O_3	CaO	Fe_2O_3	MnO	TiO_2	MgO	K_2O	Na_2O	SO_3
wt% GGBFS	31.1	13.7	40.9	0.401	0.31	1.26	9.16	0.685	0	2.31

Table 2. Mix design of AAM mixes

Mix	**GGBFS [kg/m³]**	**w/b**	**m (NaOH) - solid [kg/m3]**	**m (Na_2SiO_3)-solid [kg/m3]**	**Na_2O [wt%GGBFS]**	**Ms**	**$f_{c,28d}$ [MPa]**
S1	375	0.42	15	4.46	3.5	0.22	49.35
S2	375	0.42	15	10.09	4.1	0.42	53.76
S3	375	0.42	6.65	21.10	3.5	1.0	70.45

Mercury intrusion porosimetry (MIP) analysis was performed using the AutoPore IV 9500 2.03.00 instrument (Micromeritics Instrument), with capacity of 206 MPa. MIP was used to qualitatively compare the porosity and pore size distribution of three AAM mixes. Samples exposed to accelerated carbonation were crushed and approximately 2 g of vacuum dried samples were tested after 7 and 28 days of exposure. Unexposed samples were tested after 28 days of sealed curing and additional 14 days under laboratory conditions. The contact angle of the mercury was set at 130°.

3 Results and discussion

3.1. Carbonation depth

The results of the carbonation depth measurements are shown in Fig. 1. After 7 days of exposure to accelerated carbonation, mix S1 exhibited the highest carbonation depth, which can be explained by the lower alkali content than in the mix S2 and the lowest Ms of all three mixes [3,11,12]. Increase in Ms is expected to provide the best performance in terms of carbonation resistance due to the formation of less porous matrix structure [12]. However, mix S3, with the highest Ms = 1, but lower alkali content compared to S2, was more susceptible to carbonation than mix S2 with the highest alkali dosage and Ms = 0.42, suggesting that alkali dosage has the predominant positive impact on the carbonation resistance. In the study by Shi et al. [3], the results indicate that for Ms = 1, alkali dosage has significant influence on the carbonation depth. This influence decreases for Ms = 0.5 and Ms = 1.5, while for the Ms = 2, two mixes with alkali dosage of 6% and 8% had almost the same carbonation depth, i.e., alkali dosage had almost no influence on the increase of carbonation resistance. Based on this and the findings of this study, the increase in alkali content has the main influence on the carbonation resistance for Ms = 1, while this influence decreases for the higher Ms, and is neglectable for Ms = 2. After 28 days of exposure, S2 had the lowest carbonation depth, while the carbonation depths of S1 and S3 were almost the same. This indicates that the S3 mix has higher carbonation rate between 7 and 28 days of exposure than S1, despite the higher Ms and the same alkali content as S1. Fig. 2 shows carbonated samples of all three mixes, after 28 days.

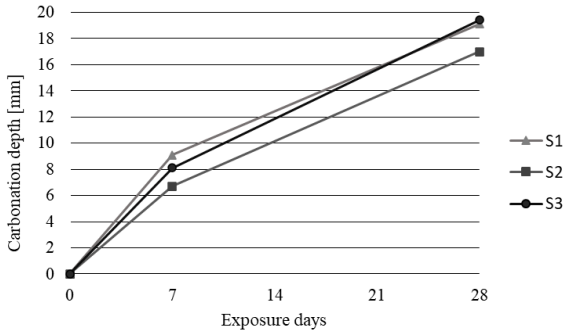

Fig. 1. Carbonation depths after 7 and 28 days of exposure to the accelerated carbonation.

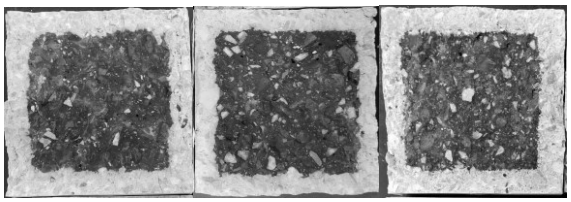

Fig. 2. Samples of the mixes S1 (a), S2 (b) and S3 (c) after 28 days of exposure to accelerated carbonation

3.2. Thermogravimetric analysis

The results of TGA analysis of unexposed samples and samples exposed for 7 and 28 days are presented in Fig. 3, Fig. 4 and Fig. 5, respectively. The first peak on the DTG curves from 30°C to 200°C is associated with the structurally unbound water and dehydration of C-A-S-H gels in all three mixes [15,16]. The peaks are less pronounced in the samples exposed for 7 days than in samples exposed for 28 days, which can be attributed to the longer decalcification time of the C-A-S-H and formation of more $CaCO_3$.

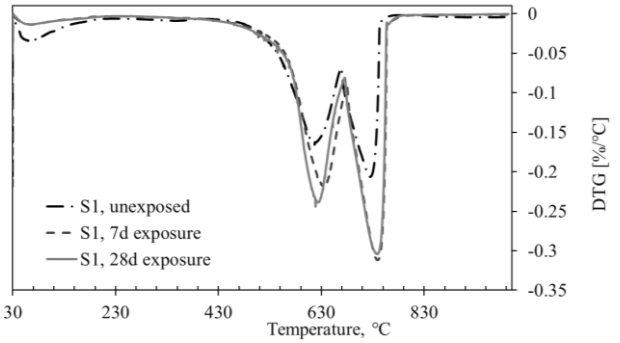

Fig. 3. DTG curves of the mix S1 - unexposed, 7 and 28 days of exposure

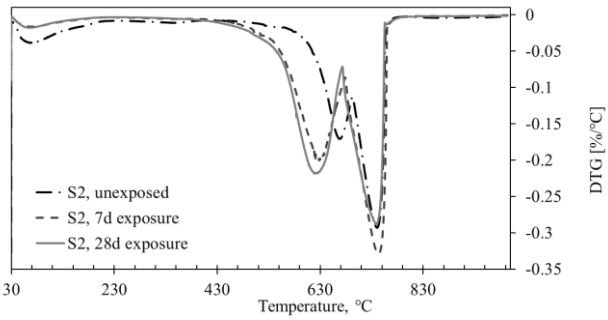

Fig. 4. DTG curves of the mix S2 - unexposed, 7 and 28 days of exposure.

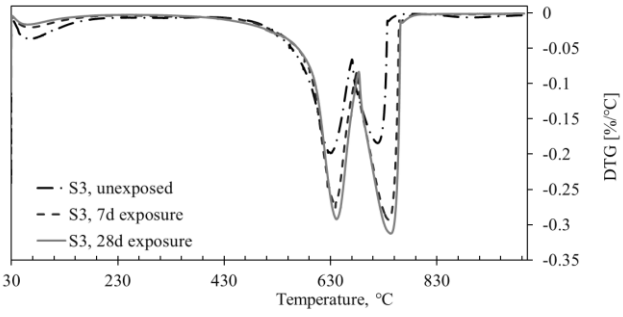

Fig. 5. DTG curves of the mix S3 - unexposed, 7 and 28 days of exposure.

Due to the layered structure of hydrotalcite, two temperature ranges can be associated with its decomposition: around 200°C and around 400°C. Therefore, the shoulder at 180°C to 200°C, and the small peak at 350°C correspond to the hydrotalcite phase (Fig. 3, Fig. 4, Fig. 5). The DTG curves of unexposed mixes S1 and S2 showed slightly higher hydrotalcite peaks than S3 (Fig. 3, Fig. 4, Fig. 5). The lowest carbonation resistance of S3 after 28 days, despite the highest Ms, could be explained by insufficient amount of alkali in the mix and less formation of CO_2 – absorbing hydrotalcite [3,14,15]. The hydrotalcite phases are less emphasised after 7 and 28 days of exposure due to conversion of hydrotalcite to $CaCO_3$. The peak between 450°C and about 700°C presents the $CaCO_3$, formed during the carbonation process. The increase in weight loss after 7 and 28 days in all three mixes shows increase in the amount of $CaCO_3$ as exposure time increases, as expected (Fig. 3, Fig. 4, Fig. 5). The temperature range from around 400°C to 670°C of $CaCO_3$ decarbonation is a consequence of the degree of crystallinity of the phase, as concluded in [3], which can also be an explanation for the shifted peaks (e.g., unexposed S2, Fig. 4), where the shift towards the higher temperatures indicates formation of less amorphous phases (e.g., Fig. 4, S2, unexposed compared to exposed samples). Peaks between 670°C and 770°C correspond to weight loss of dolomite aggregate and are not analysed further in this study.

The shift of the S3 DTG $CaCO_3$ peaks compared to S1 and S2 could indicate that more silica content in the AAM binders tends to form $CaCO_3$ of higher crystallinity, as stated before. The highest amount of $CaCO_3$ is formed in the S3 sample, and the lowest in S2, which corresponds to the higher content of C-A-S-H gel formed.

3.3. Mercury intrusion porosimetry

The results of the MIP analysis are presented in Fig. 6, Fig. 7, Fig. 8 and Fig. 9. Although there are some reports in the literature about decreased porosity after carbonation of NaOH activated slag [3], the porosity of three mixes increased after 28 days of accelerated carbonation (Fig. 6 and Fig. 7).

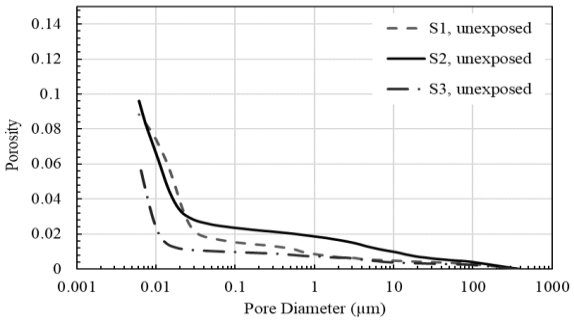

Fig. 6. Total porosity of S1, S2 and S3 mixes before exposing to accelerated carbonation

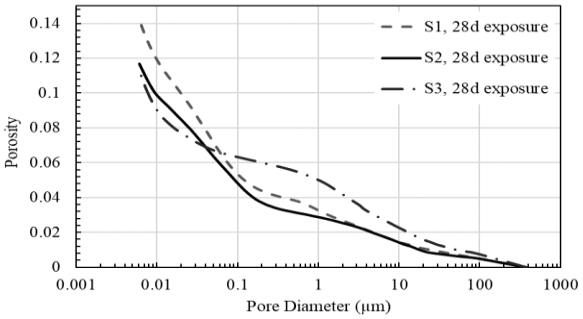

Fig. 7. Total porosity of S1, S2 and S3 mixes after 28 days of exposure to accelerated carbonation

However, mix S2 had the lowest relative increase (21.4%), while mixes S1 and S3 showed a similar increase (S1 – 60.7% and S3 – 61.2%, respectively). This can be explained by the higher Na_2O content in S2 compared to S1 and S3, leading to the formation of more hydrotalcite phase during hydration and filling the pores due to its expansion [13].

After carbonation, the pore volume increased in the range between 0.6 and 30 μm, (Fig. 8 and Fig. 9), most significantly in S3, which increased the permeability and therefore the carbonation rate of the mix [17]. In the micro capillary pore region, between 0.01 and 0.3 μm, S1 and S2 had the highest increase in pore volume. While the S2 and S3 mixes showed decrease in gel pores (<0.01 μm) volume, the pore volume of S1 increased in this range. A higher average porosity after carbonation and coarsening of the pores is present in all mixes and it is attributed in the literature to the decalcification of the C-A-S-H gel [3].

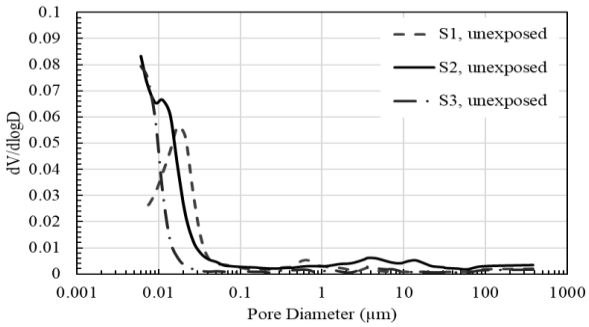

Fig. 8. Log differential curve of S1, 2 and 3 mixes before exposing to accelerated carbonation

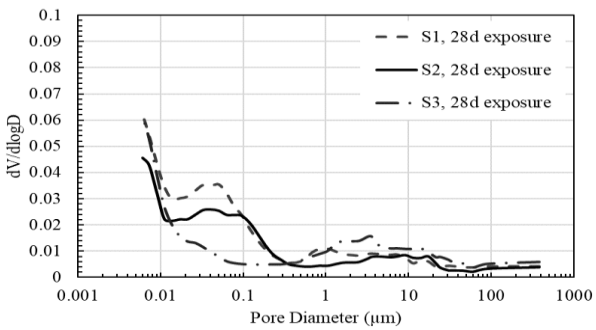

Fig. 9. Log differential curves of S1, 2 and S3 mixes after 28 days of exposure to accelerated carbonation.

4 Conclusions

This paper presents the results of the analysis of the carbonation resistance and microstructural changes of three alkali-activated slag concrete mixes, exposed to accelerated carbonation with 3% CO_2 at 20°C and RH 57%. The main conclusions that can be withdrawn are:

- Although higher Ms leads to formation of a denser matrix, alkali dosage has a significant influence on the increase of carbonation resistance.
- Higher alkali content tends to form more hydrotalcite, which acts like a CO_2 absorbent and increases the carbonation resistance.
- Accelerated carbonation leads to an increase in total porosity and coarsening of the pores in AAMs. The mix with the highest alkali content had the lowest relative increase in porosity, possibly due to the formation of more hydrotalcite, which has the pore-filling effect, due to its expansion. The mix with the highest Ms had the smallest increase in micro capillary pore volume, but the highest increase in the pore volume in the 0.6 and 30 μm range, which may be the reason for its increased susceptivity to carbonation.

Acknowledgement

This research has been conducted as a part of the project DuRSAAM - The PhD Training Network on Durable, Reliable and Sustainable Structures with Alkali-Activated Materials funded by the European Union's Horizon 2020 research and innovation programme under the Marie Skłodowska-Curie grant agreement No 813596. Second author is acknowledging the support of the project "Alternative Binders for Concrete: understanding microstructure to predict durability, ABC", funded by the Croatian Science Foundation under number UIP-05-2017-4767.

References

[1] Ramagiri KK, Kar A. Environmental impact assessment of alkali-activated mortar with waste precursors and activators. Journal of Building Engineering,2021;44:103391.

[2] Provis JL. Geopolymers and other alkali activated materials: why, how, and what? Mater Struct 2014;47:11–25.

[3] Shi Z, Shi C, Wan S, Li N, Zhang Z. Effect of alkali dosage and silicate modulus on carbonation of alkali-activated slag mortars. Cement and Concrete Research 2018;113:55–64.

[4] Provis JL, van Deventer JSJ, editors. Alkali Activated Materials - State of the Art Report TC 224-AAM. vol. 13. Dordrecht: Springer Netherlands; 2014.

[5] Gruskovnjak A, Lothenbach B, Holzer L, Figi R, Winnefeld F. Hydration of alkali-activated slag: comparison with ordinary Portland cement. Advances in Cement Research 2006;18:119–28.

[6] Ben Haha M, Le Saout G, Winnefeld F, Lothenbach B. Influence of activator type on hydration kinetics, hydrate assemblage and microstructural development of alkali activated blast-furnace slags. Cement and Concrete Research 2011;41:301–10.

[7] Puertas F, Palacios M, Manzano H, Dolado JS, Rico A, Rodríguez J. A model for the C-A-S-H gel formed in alkali-activated slag cements. Journal of the European Ceramic Society 2011;31:2043–56.

[8] Bernal SA, Provis JL, Brice DG, Kilcullen A, Duxson P, van Deventer JSJ. Accelerated carbonation testing of alkali-activated binders significantly underestimates service life: The role of pore solution chemistry. Cement and Concrete Research 2012;42:1317–26..

[9] Wang A, Zheng Y, Zhang Z, Liu K, Li Y, Shi L, et al. The Durability of Alkali-Activated Materials in Comparison with Ordinary Portland Cements and Concretes: A Review. Engineering 2020;6:695–706.

[10] Zhang J, Shi C, Zhang Z. Carbonation induced phase evolution in alkali-activated slag/fly ash cements: The effect of silicate modulus of activators. Construction and Building Materials 2019;223:566–82.

[11] Bernal SA. Effect of the activator dose on the compressive strength and accelerated carbonation resistance of alkali silicate-activated slag/metakaolin blended materials. Construction and Building Materials 2015;98:217–26.

[12] Zhang X, Long K, Liu W, Li L, Long W-J. Carbonation and Chloride Ions' Penetration of Alkali-Activated Materials: A Review. Molecules 2020;25:5074.

[13] Jing Li, Chaofan Yi, Zheng Chen, Wenxiang Cao, Suhong Yin, Haoliang Huang, et al. Relationships between reaction products and carbonation performance of alkali-activated slag with similar pore structure 2022;45.

[14] Bernal SA, San Nicolas R, Myers RJ, Mejía de Gutiérrez R, Puertas F, van Deventer JSJ, et al. MgO content of slag controls phase evolution and structural changes induced by accelerated carbonation in alkali-activated binders. Cement and Concrete Research 2014;57:33–43.

[15] Charitha V, Athira G, Bahurudeen A, Shekhar S. Carbonation of alkali activated binders and comparison with the performance of Ordinary Portland cement and blended cement binders. Journal of Building Engineering 2022;53.

[16] Park SM, Jang JG, Lee HK. Unlocking the role of MgO in the carbonation of alkali-activated slag cement. Inorg Chem Front 2018;5:1661–70. https://doi.org/10.1039/C7QI00754J.

[17] Mehta PK, Monteiro PJM. Concrete: microstructure, properties, and materials. 3rd ed. New York: McGraw-Hill; 2006.